[CANCER RESEARCH 64, 1959–1965, March 15, 2004]

# Brca2 Deficiency Does Not Impair Mammary Epithelium Development but Promotes Mammary Adenocarcinoma Formation in *p53*$^{+/-}$ Mutant Mice

**Alison M. Y. Cheung,[1,2] Andrew Elia,[1] Ming-Sound Tsao,[2] Susan Done,[2] Kay-Uwe Wagner,[3] Lothar Hennighausen,[4] Razqallah Hakem,[1,2] and Tak W. Mak[1,2]**

*[1]Advanced Medical Discovery Institute, Toronto, Ontario, Canada; [2]Ontario Cancer Institute and Department of Medical Biophysics, University of Toronto, Toronto, Ontario, Canada; [3]Eppley Institute for Research in Cancer and Allied Diseases, University of Nebraska Medical Center, Omaha, Nebraska; and [4]Laboratory of Genetics and Physiology, National Institute of Diabetes, Digestive and Kidney Diseases, NIH, Bethesda, Maryland*

## ABSTRACT

**Brca2 is an important tumor suppressor associated with susceptibility to breast cancer. Although increasing evidence indicates that the primary function of Brca2 is to facilitate the repair of DNA damage via the homologous recombination pathway, how Brca2 prevents breast cancer is largely unknown. To study the role of Brca2 specifically in mammary epithelium development, we crossed mice bearing the conditionally deficient allele *Brca2*$^{flox9-10}$ to mouse mammary tumor virus- or whey acidic protein-*Cre* transgenic lines. Analysis of these animals showed that Brca2 is not required for epithelial expansion in mammary glands of pregnant mice. In addition, examination of mammary gland involution revealed normal kinetics of mammary alveolar cell apoptosis after weaning of litters. Nevertheless, Brca2-deficient mice developed mammary adenocarcinomas after a long latency (average, 1.6 years). Detailed histopathological analysis of four of these tumors demonstrated that three of them showed abnormal p53 protein expression. A mutation in the *p53* gene was detected in one case. Moreover, homozygosity *versus* heterozygosity for the Brca2 mutation heavily skewed the tumor spectrum toward mammary adenocarcinoma development in *p53*$^{+/-}$ mice. Our data indicate that Brca2 is not essential for mammary epithelium development but that Brca2 deficiency and down-regulated p53 expression can work jointly to promote mammary tumorigenesis.**

## INTRODUCTION

The identification and cloning of the breast cancer susceptibility genes *BRCA1* and *BRCA2* genes has revealed the molecular basis of the majority of hereditary breast cancers in women (1, 2). Although the two *BRCA* genes are not homologous in sequence, they have similar expression patterns during cell cycle progression and in embryonic (3) and adult (1, 4, 5) tissues. Numerous biochemical studies of the human BRCA proteins have shown that both gene products are regulators of cellular genomic stability. Whereas BRCA1 has additional functions in transcription regulation, the control of centrosome number, and ubiquitination (for a recent review, see Ref. (6), the major identified function of BRCA2 is to bind to Rad51 and regulate the activity of this molecule during homology-directed recombination repair of DNA double-strand breaks (7). On one hand, the BRC repeats of BRCA2 (which mimic the oligomerization domain of Rad51 in structure) bind to Rad51 (8) and prevent it from binding to single-stranded DNA to form nucleoprotein complexes. Rad51-mediated DNA repair activity is thus inhibited (9). On the other hand, a different region near the COOH terminus of BRCA2 binds single-stranded DNA and stimulates Rad51-mediated recombination *in vitro* (10). In addition, it was recently shown that the portion of the BRCA2 protein encoded by exon 3 binds to a novel protein called EMSY, an interaction that leads to the silencing of BRCA2-mediated transcriptional activation (11). Animal studies have also supported a role for BRCA2 in controlling genomic stability. Murine cells, which completely lack Brca2 or express a truncated form of Brca2, have a proliferative defect characterized by increased expression of the tumor suppressor gene p53 and its transcriptional target p21$^{WAF1/Cip1}$. Brca2-deficient cells are also more sensitive to apoptosis induced by DNA-damaging agents (12–15).

Although the biochemical function of BRCA2 is now known, how it acts as a tumor suppressor in human breast and ovarian cancers is still a mystery. Mutations in BRCA2 contribute to 32% of hereditary breast cancers in women and to 14% in men (16). In mice, mammary epithelium that lacks Brca2 expression undergoes cancerous transformation after a long latency (17), and tumor cells in this tissue exhibit genomic instability. Furthermore, simultaneous loss of Brca2 and p53 in epithelial tissues drastically increases the incidence of skin and mammary tumors (18). However, the involvement of Brca2 in normal mammary epithelium development has not been investigated. Morphogenesis of the mammary gland occurs in several stages, starting with a fetal anlage, which undergoes ductal elongation and branching (19). During puberty, the ductal tree undergoes additional branching to expand throughout the fat pad. However, maximal expansion and proliferation of the ductal and alveolar epithelia to generate a fully functional mammary gland with secretory lobulo-alveolar structures does not occur until pregnancy. After weaning, the mammary gland involutes via massive apoptosis of epithelial cells that returns the gland to its prepregnant-like state. These processes are stringently regulated by steroid and peptide hormones (20). Expression studies have demonstrated that BRCA2 is up-regulated in response to the steroid and growth hormones that induce mammary epithelial cell proliferation during pregnancy (3). However, whether BRCA2 is involved in normal mammary epithelium development remains to be defined, as does the potential role of this protein in mammary cell proliferation during pregnancy and/or apoptosis during involution.

To address these questions, we took advantage of previously generated *Brca2*$^{flox9-10}$ mice in which *Brca2* exons 9–10 are floxed (flanked by loxP; Ref. 21). We crossed *Brca2*$^{flox9-10}$ mice with *MMTV-Cre* or *WAP-Cre* transgenic mice to produce mutants that specifically lack Brca2 at different stages of mammary gland development. In *WAP-Cre* transgenic mice, Cre recombinase is induced only during late pregnancy and lactation (22, 23). In *MMTV-Cre* transgenic mice, the mouse mammary tumor virus (MMTV) long terminal repeat promoter drives the expression of Cre recombinase in mammary epithelium (among other tissues) before puberty (22, 23). The generation of these mutant animals allowed us to examine the effect of Brca2 deficiency at critical points of mammary gland development and tumorigenesis.

## MATERIALS AND METHODS

**Generation of Mammary Gland-Specific Brca2-Deficient Mice.** The generation of mice bearing a floxed allele of *Brca2* exons 9–10 (*Brca2*$^{fl9-10}$) has been described previously (21). To inactivate Brca2 specifically in mammary epithelium, *Brca2* $^{fl9-10/+}$ mice were crossed to *MMTV-Cre* transgenic mice (22) expressing Cre recombinase under the control of MMTV long

Received 7/24/03; revised 12/22/03; accepted 1/6/04.

The costs of publication of this article were defrayed in part by the payment of page charges. This article must therefore be hereby marked *advertisement* in accordance with 18 U.S.C. Section 1734 solely to indicate this fact.

**Requests for reprints:** Tak W. Mak, Advanced Medical Discovery Institute, University Health Network, 620 University Avenue, Suite 706, Toronto, Ontario, M5G 2C1 Canada. Phone: (416) 946-2234; Fax: (416) 204-5300; E-mail: tmak@uhnres.utoronto.ca.

terminal repeat promoter or to *WAP-Cre* transgenic mice (22) expressing Cre recombinase under the control of the whey acidic protein (WAP) promoter. The resulting mutant mice (*Brca2*$^{fl9-10/fl9-10}$*; MMTV-Cre* and *Brca2*$^{fl9-10/fl9-10}$*; WAP-Cre*) were analyzed in both 129/C57BL/6 and FVB/C57BL/6 genetic backgrounds. Mammary glands collected from a total of 68 129/C57BL/6 and 20 FVB/C57BL/6 mice of various Brca2 and Cre genotypes were used for whole mount, histological, terminal deoxynucleotidyl transferase-mediated nick end labeling, and Southern and Western analyses as described below. No phenotypic differences were observed between genetic backgrounds. For timed pregnancies, male and female mice were mated overnight, and females were scored for vaginal plaques the next morning. The presence of vaginal plaques was taken to represent pregnancy day0.5. *Brca2*$^{fl9-10/fl9-10}$*; MMTV-Cre* and *Brca2*$^{fl9-10/fl9-10}$*; WAP-Cre* mice were also crossed to *p53*$^{+/-}$ mice (Taconic) to produce *Brca2*$^{fl9-10/fl9-10}$*; MMTV-Cre; p53*$^{+/-}$ and *Brca2*$^{fl9-10/fl9-10}$*; WAP-Cre; p53*$^{+/-}$ mice. All experiments were performed in compliance with the guidelines of the Ontario Cancer Institute Animal Care Committee.

**Induction of Involution and Mammary Tissue Collection.** Litter size was kept at 5 pups to equalize suckling frequency on each teat and to minimize variation between mice. To induce involution, pups were removed at day 10 after birth (d10L). Day 1 of involution (d1i) began 24 h after pup removal, with all subsequent days being designated accordingly. For mammary tissue collection, one of the abdominal mammary glands was fixed in 10% buffered formalin (Fisher Scientific, Nepean, Ontario, Canada), whereas the other was saved for whole mount analysis (see below). The first or second thoracic mammary glands were collected and a portion of the tissue was digested in tissue lysis buffer (10 mM Tris, 1 mM EDTA, 0.1 M NaCl, 1%SDS, and 0.2 mg/ml proteinase K) and subjected to phenol/chloroform extraction to obtain genomic DNA for Southern blotting. Another portion was used for protein immunoblotting (see below).

**Southern Blotting and PCR Analysis.** Genomic DNA was prepared from mammary tissue or tumor tissue following standard protocols. For Southern blots, 20 $\mu$g of DNA digested with *Bam*HI were blotted and hybridized to a probe derived from *Brca2* exon 8 that was able to distinguish between the recombined and nonrecombined floxed Brca2 alleles (21). Levels of recombination were assessed using the volume quantitation tools of ImageQuant software (Amersham Biosciences). Volume quantitation is calculated based on the pixel intensity of the band created by the hybridization of a defined probe to the restriction fragments representing the recombined or nonrecombined alleles. To detect recombination of the floxed allele using PCR, the primer set 5′-GCTAAATTTAATTGTTTTACAGCC-3′ and 5′-TACACAGGGTTCT-CACCAAAC-3′ was used. PCR was performed at the annealing temperature of 61°C for 40 cycles. A PCR product of 450 bp was expected when Brca2 exons 9 and 10 were successfully excised.

**Whole Mount Preparation.** Abdominal mammary glands harvested as above were placed onto microscope glass slides and fixed overnight in Carnoy's solution (3:1 ethanol:glacial acetic acid). After dehydration with 70% ethanol for 30 min, the samples were stained overnight in carmine alum [0.2% carmine dye (Sigma) and 0.5% aluminum potassium sulfate (Sigma)]. Destaining was performed with 2% hydrochloric acid in 70% ethanol. The samples were then dehydrated gradually in increasing concentrations of ethanol and cleared in Toluene (Caledon) and examined under the light microscope at low (×8) and high (×40) magnifications.

**Histological Analysis.** Mice in distress or exhibiting obvious tumors were sacrificed and subjected to histopathological evaluation. For detection of hyperplasias, mice were sacrificed, and all second thoracic and abdominal mammary glands were harvested. Tissues and tumors were fixed in 10% buffered formalin and routinely processed for paraffin embedding. Sections (3 $\mu$m) were prepared and stained with H&E. Immunohistochemistry using an anti-p53 antibody (CM5; Novacastra) was performed using the microwave antigen retrieval and avidin-biotin methods. Incubation with the primary antibody was performed at 1:500 for 2 h at room temperature. After washing in PBS, the sections were incubated with biotin-conjugated antirabbit IgG antibodies for 45 min, followed by the treatment with the Vectastain ABC system and the DAB kit (both from Vector Laboratories, Inc., Burlingame CA). Sections were counterstained in hematoxylin and mounted using Entellan (Merck, Darmstadt, Germany).

**Apoptosis Assays.** Terminal deoxynucleotidyl transferase-mediated nick end labeling assays were performed on 3-$\mu$m tissue sections using the *In Situ* Cell Death Detection kit (Roche Diagnostics GmbH) following manufacturer's protocol. Processed sections were then examined using a fluorescence microscope, and positively stained cells in three fields were counted.

**Western Blotting.** Whole cell lysates were prepared from mammary glands using radioimmunoprecipitation assay lysis buffer [20 mM Tris (pH 7.5), 2 mM EDTA, 1% sodium deoxycholate, 150 mM NaCl, 0.25% SDS, and 1% Triton X-100]. Lysates (20 $\mu$g) were fractionated by SDS-PAGE and transferred to nitrocellulose for immunoblotting. Antibodies reactive to cleaved caspase-3 (Asp$^{175}$; Cell Signaling Technology) or $\beta$-actin (Sigma) were used according to manufacturers' protocols.

**Analyses of p53 Mutations and Loss of Heterozygosity.** Mutations in *p53* exons 5–9 in tumors were detected by microsequencing methods. Where genomic DNA from tumors was available, PCR primers designed to amplify each exon were used with the Expand High Fidelity PCR System (Roche Diagnostics GmbH, Lebach, Germany) at the optimized annealing temperature according to manufacturer's protocol. Where RNA from tumors was available, cDNA was generated using the Sensiscript RT kit (Qiagen). Primers designed to amplify 1173 bp of *p53* cDNA were used with the Expand High Fidelity PCR System at the optimized annealing temperature. The PCR products were then cloned into the pCR2.1 vector using the TA cloning kit (Invitrogen) according to manufacturer's protocol. The cloned plasmids were sequenced and examined for *p53* mutations. To detect loss of heterozygosity of p53 in *p53*$^{+/-}$ mice, genomic DNA obtained from tumors or selected tissues was digested with *Bam*HI and subjected to Southern blotting using a previously described probe for p53 exons 2–6 (24). Loss of the hybridization signal from the wild-type (WT) p53 fragment in tumor cells, as compared with the hybridization signals of WT and mutant fragments from normal tissues of the same p53$^{+/-}$ mouse, was taken as evidence of loss of heterozygosity.

**Statistical Analysis.** Survival curves of mice were analyzed with the statistical software Prism, which uses a log-rank test to determine statistically significant differences between tumor-free survival curves of different mice. The spectrum of tumors developed was also analyzed with the Prism software, which uses a $\chi^2$ test for contingency table analysis.

## RESULTS

**Cre-Mediated Recombination of Brca2$^{fl9-10}$ in Mammary Tissue.** To quantify the extent of Cre-mediated recombination of the floxed *Brca2* allele in *Brca2*$^{fl9-10/fl9-10}$*; WAP-Cre* mice, we collected genomic DNA from mammary tissues and performed Southern blotting using a previously described probe (21). This probe binds to exon 8 of *Brca2* and distinguishes between the nonrecombined (*Brca2*$^{fl9-10}$) and recombined (*Brca2*$^{\Delta 9-10}$) alleles. To compare the level of recombination of the floxed allele between heterozygous and homozygous *Brca2*$^{fl9-10}$ mice, we performed densitometric quantitation of the pixel intensities of the restriction fragment bands within the rectangles indicated in Fig. 1*A–C*. We then calculated the percentage of total floxed alleles that had recombined: [volume of the recombined allele (*Δ9–10*)/volume of (recombined + nonrecombined(*fl9–10*) or WT allele) × 100%]. We observed a low level of recombination (9.99%) in cells from the mammary glands of d16.5 pregnant *Brca2*$^{fl9-10/fl9-10}$*; WAP-Cre* mice, which was nevertheless double the level of recombination observed in *Brca2*$^{fl9-10/+}$*; WAP-Cre* females at the same stage of pregnancy (4.48%; Fig. 1*A*). Because the genomic DNA had been collected from whole fat pads, this modest level of recombination may reflect the relatively low number of epithelial cells present in this tissue. A higher level of recombination (20.86%) was observed in *Brca2*$^{fl9-10/fl9-10}$*; WAP-Cre* mice by several hours postpartum (Fig. 1*B*), consistent with the normal activation of the *WAP* promoter during late pregnancy and lactation (22). This level of recombination is consistent with that observed for mice with a mammary epithelium-specific mutation of Brca1 (*Brca1*$^{Ko/Co}$*Wap-Cre* mice; Ref. 25). By day 21 postweaning, 25.10% of cells in the mammary tissue of *Brca2*$^{fl9-10/fl9-10}$*; WAP-Cre* mice showed recombination of the floxed allele (Fig. 1*C*), suggesting that Brca2-deficient

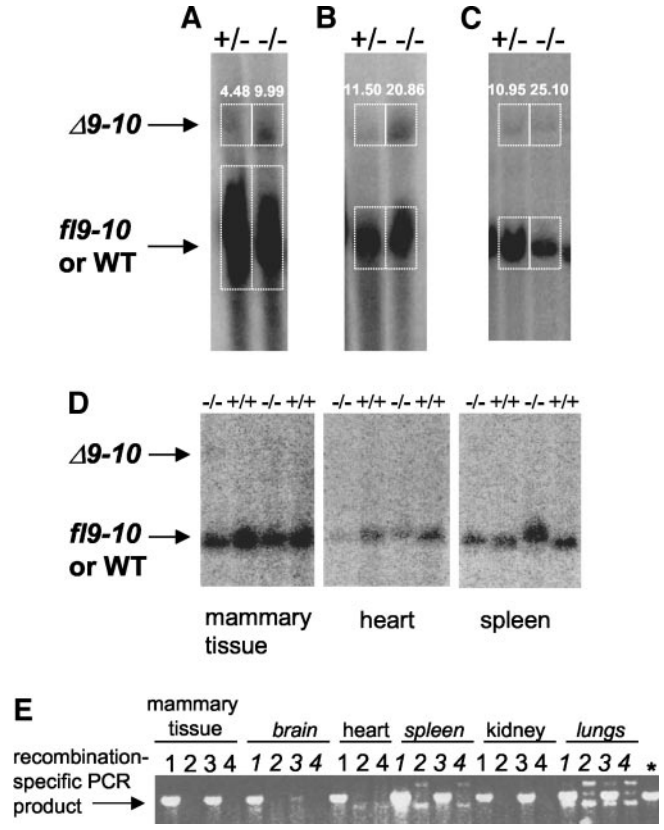


Fig. 1. Recombination of the *Brca2*$^{fl9-10}$ allele in the mammary epithelium of *Brca2*$^{fl9-10/fl9-10}$*; WAP-Cre* and *Brca2*$^{fl9-10/fl9-10}$*; MMTV-Cre* mice. *A–C,* genomic DNA obtained from whole mammary tissues of *Brca2*$^{fl9-10/fl9-10}$*; WAP-Cre* (−/−) or control (+/−) mice at different developmental stages were analyzed by Southern blotting using a *Brca2* exon 8 probe. The volume quantitation method (see "Materials and Methods") was used to compare the pixel intensities of the Δ9–10 and *fl9–10* or WT alleles within the indicated rectangular boxes of each sample. The percent recombination was calculated as [volume of Δ9–10/total (Δ9–10+ *fl9–10*) volume × 100%] as indicated over the top of each rectangle. *A,* day 16 of pregnancy. *B,* 4–6 h postpartum. *C,* day 21 postweaning of the first litter of pups. *D–E,* levels of recombination of the *Brca2*$^{fl9-10}$ allele in *Brca2*$^{fl9-10/fl9-10}$*; MMTV-Cre* mice. *D,* Southern blotting of genomic DNA obtained from mammary tissue, heart, or spleen of virgin *Brca2*$^{fl9-10/fl9-10}$*; MMTV-Cre* (−/−) or WT (+/+) mice. The Δ9–10 allele was barely detectable in mammary tissue of −/− mice. *E,* PCR of genomic DNA obtained from the indicated tissues of: mouse 1, *Brca2*$^{fl9-10/fl9-10}$*; MMTV-Cre*; mouse 2, *Brca2*$^{fl9-10/+}$; mouse 3, *Brca2*$^{fl9-10/fl9-10}$*; MMTV-Cre*; mouse 4, wild type (WT) and ∗, positive control. The recombination of the *fl9–10* allele has occurred in multiple tissues of Brca2-deficient mice. Results shown are representative of two experiments each using a total number of 3 mice/genotype.

epithelial cells can survive after involution despite the ensuing massive apoptosis of lobulo-alveolar cells.

We also investigated levels of recombination of the floxed allele in the mammary tissue of *Brca2*$^{fl9-10/fl9-10}$*; MMTV-Cre* mice using Southern blotting and PCR (Fig. 1, *D–E*). Recombination of the *Brca2*$^{fl9-10}$ allele in cells of virgin mammary tissue of these animals was almost undetectable using Southern blotting (Fig. 1*D*). To investigate whether recombination could be detected using PCR, we carried out amplifications using primers that bound to either the intron between exons 7 and 8 or the intron between the LoxP site and exon 11. A product of size 450 bp was expected if exons 9 and 10 were successfully removed from the floxed *Brca2* allele. As shown in Fig. 1*E*, the recombined *Brca2*$^{\Delta 9-10}$ allele was detected in all tissues examined in 2 *Brca2*$^{fl9-10/fl9-10}$*; MMTV-Cre* mice (Fig. 1*E*, *Lanes 1* and *3*). These data indicate that a low but detectable level of recombination of the *Brca2*$^{fl9-10}$ allele gives rise to at least a few Brca2-deficient cells in the mammary tissue of *Brca2*$^{fl9-10/fl9-10}$*; MMTV-Cre* mice. The observation that Brca2 recombination had also occurred in a number of other tissues is in agreement with the previously reported leakiness of this transgenic line (23).

**Normal Ductal and Alveolar Epithelium Proliferation in Pregnant Brca2$^{fl9-10/fl9-10}$; WAP-Cre Mice.** *Brca1*$^{Ko/Co}$*Wap-Cre* mice show a defect in mammary ductal tree expansion during pregnancy that is accompanied by increased apoptosis, suggesting that WT Brca1 is required for normal mammary cell proliferation and ductal tree morphogenesis (25). Embryonic cells from mice with a homozygous truncation mutation of Brca2 also demonstrate a block in proliferation in association with enhanced expression of p53 and p21 proteins (12). To determine whether Brca2 is required for the proliferation of mammary epithelial cells, we examined whole mount preparations of mammary glands from pregnant *Brca2*$^{fl9-10/fl9-10}$*; WAP-Cre* and control mice (Fig. 2). Expansion of the ductal and alveolar epithelium during pregnancy depends on the signaling of both peptide and steroid sex hormones. Day 16 pregnant *Brca2*$^{fl9-10/fl9-10}$*; WAP-Cre* mice were just as competent as heterozygous controls at expanding the ductal trees and forming lobulo-alveolar structures, suggesting that Brca2 is not required for mammary epithelial cell proliferation (Fig. 2, *A* and *B*). We also examined the mammary ductal trees from mutant and control mice at several hours postpartum (Fig. 2, *C* and *D*). Again, the proliferation of Brca2-deficient epithelial cells appeared to be normal. A similar study using mammary tissue from *Brca2*$^{fl9-10/fl9-10}$*; MMTV-Cre* mutant mice also showed normal proliferation at day 16 of pregnancy and postpartum (data not shown).

**Brca2-Deficient Mammary Epithelial Cells Demonstrate Normal Kinetics of Apoptosis during Involution.** Embryonic cells from Brca2-null or Brca2 truncation mutant mice demonstrate increased sensitivity to DNA-damaging stress (12, 13). Similarly, activated T lymphocytes from mice with a T-cell-specific mutation of Brca2 (*Brca2*$^{fl9-10/fl9-10}$*; Lck-Cre* mice) exhibit an elevated level of spontaneous cell death (21). These observations can probably be attributed to the involvement of Brca2 in the regulation of DNA damage repair. DNA

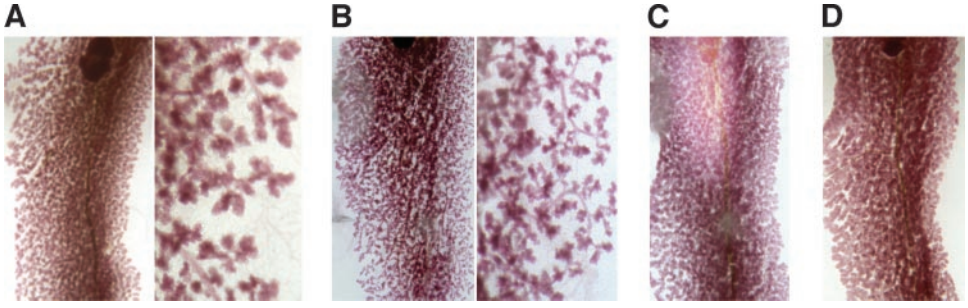


Fig. 2. Normal expansion and proliferation of mammary epithelium in the absence of Brca2. *A,* whole mount analysis of the abdominal mammary gland from a day 16 pregnant *Brca2*$^{fl9-10/fl9-10}$*; WAP-Cre* mutant mouse stained with carmine alum and viewed at ×8 magnification (*left panel*). A higher magnification (×25) shows apparently normal development of lobulo-alveolar structures (*right panel*). *B,* mammary gland from a *Brca2*$^{fl9-10/+}$*; WAP-Cre* control analyzed as in *A*. *C* and *D,* whole mount analysis of the abdominal mammary glands from a *Brca2*$^{fl9-10/fl9-10}$*; WAP-Cre* mouse (*C*) and a *Brca2*$^{fl9-10/+}$*; WAP-Cre* mouse (*D*) at 4–6 h postpartum. Results shown are representative of two experiments each using a total of 3 mice/genotype.

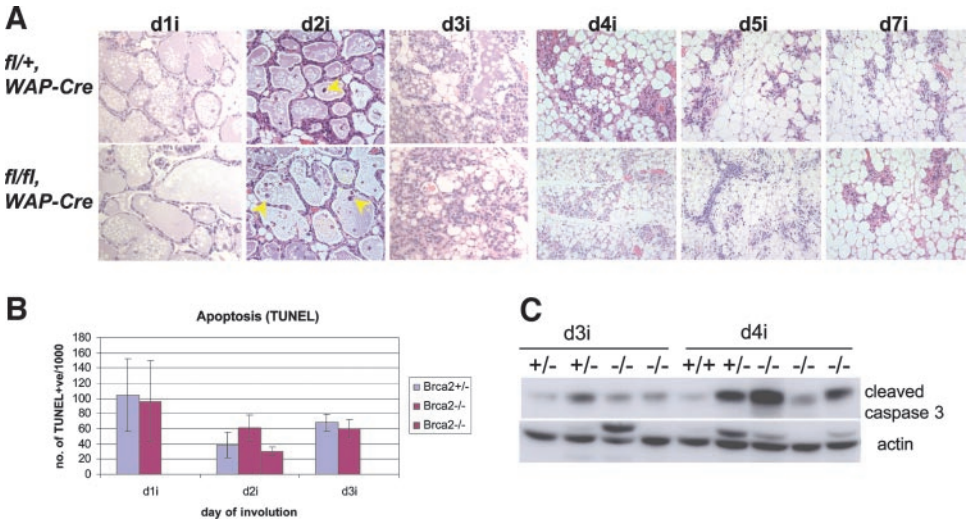


Fig. 3. Normal mammary gland involution in the absence of Brca2. *A*, H&E staining of tissue sections from involuting glands of *Brca2*$^{fl9-10/+}$*; WAP-Cre* (*top panels*) and *Brca2*$^{fl9-10/fl9-10}$*; WAP-Cre* (*bottom panels*) mice. Day 1 of involution (d1i) indicates the first day of involution, and the following days are denoted accordingly. *Arrows* in d2i indicate apoptotic cells shed into the alveolar lumens. At d3i, adipose tissue starts to reconstitute the fat pad and epithelial cells surrounding the lumen regress into epithelial cords. By d7i, the mammary glands have finished regressing and have returned to a virgin, prepregnant-like state. Results shown are representative of three experiments using at least 3 mice/genotype. *B*, quantification of apoptotic cells using terminal deoxynucleotidyl transferase-mediated nick end labeling (TUNEL) assays. Results shown are the mean ± SD of numbers of TUNEL-positive cells/1000 cells counted from three different fields. *C*, apoptosis measured by the level of cleaved (activated) caspase-3. Whole protein lysates (20 $\mu$g) prepared from mammary glands of *Brca2*$^{fl9-10/+}$*; WAP-Cre* (+/−) or *Brca2*$^{fl9-10/fl9-10}$*; WAP-Cre* (−/−) mice at d3i or d4i were immunoblotted to detect cleaved caspase-3. Results shown are representative of three independent experiments.

aberrations accumulate in cells proliferating in the absence of Brca2, which in turn activates the apoptotic machinery. To determine whether proliferating Brca2-deficient mammary epithelial cells were also sensitized to apoptosis, we studied involution in *Brca2*$^{fl9-10/fl9-10}$*; WAP-Cre* and control *Brca2*$^{fl9-10/+}$*; WAP-Cre* mice (Fig. 3). Analysis of H&E-stained sections from control mammary glands obtained at various days after forced weaning of pups revealed morphological changes that started as early as the first day of involution (d1i; Fig. 3*A*). Epithelial cells lining the milk-containing alveoli of control mice started to be shed into the lumens, a trend more noticeable by day2i. By day 3 of involution, the alveoli had almost completely collapsed and adipose tissue had begun to reconstitute the fat pad. This process continued until day7i when the gland completed its regression and returned to the prepregnant-like state. Notably, the morphological changes in *Brca2*$^{fl9-10/fl9-10}$*; WAP-Cre* mammary tissue were indistinguishable in pattern and kinetics from those of the *Brca2*$^{fl9-10/+}$*; WAP-Cre* controls. We then quantified the level of apoptosis by terminal deoxynucleotidyl transferase-mediated nick end labeling assay. Comparable levels of terminal deoxynucleotidyl transferase-mediated nick end labeling-positive cells were detected at d1i, d2i, and d3i in the involuting mammary glands of both mutant and control mice (Fig. 3*B*), suggesting that Brca2 deficiency does not affect involution in mouse mammary glands. This conclusion was additionally confirmed by analysis of activated caspase-3 in whole cell lysates prepared from involuting glands (Fig. 3*C*). Activated caspase-3 was not detectable before day 3 of involution (data not shown), consistent with a previous study (26). Analyses of several samples from d3i and d4i *Brca2*$^{fl9-10/+}$*; WAP-Cre* and *Brca2*$^{fl9-10/fl9-10}$*; WAP-Cre* mammary tissues demonstrated considerable variation but no reproducible differences in levels of cleaved caspase-3.

**p53 Status in Spontaneous Mammary Adenocarcinomas of Brca2-Deficient Mice.** Despite the normal development of mammary tissue in Brca2-deficient mice, 4 of 6 *Brca2*$^{fl9-10/fl9-10}$*; MMTV-Cre* female mice developed spontaneous mammary adenocarcinomas after a long latency (average 1.6 years; Table 1). Pathological evaluation was done according to the guidelines in the consensus report from the Annapolis meeting on the mammary pathology of genetically engineered mice (27). This latency period is comparable with the latency of 1.4 years previously reported for mammary adenocarcinoma development in *Brca2*$^{flox/-}$*; Wap*$^{cre/+}$ mice (17). Southern blotting indicated that the recombination of both *Brca2*$^{fl9-10}$ alleles occurred in almost all tumor cells, suggesting that mutation of Brca2 is responsible for the cancerous transformation of mammary cells (Fig. 4*A*). These data also suggest that, although there were few cells in the mammary tissue of *Brca2*$^{fl9-10/fl9-10}$*; MMTV-Cre* mice with a deletion of Brca2 exons 9 and 10, these cells were sufficient to initiate tumorigenesis.

Several lines of evidence have indicated that p53 signaling is often abrogated in human BRCA-associated breast cancers (28). In a mouse model, simultaneous loss of *Brca2* and *p53* in the epithelium acted synergistically to accelerate the development of breast

Table 1 *Development of spontaneous tumors in Brca2*$^{fl9-10/fl9-10}$*; MMTV-Cre female mice*

The pathology of mammary adenocarcinomas were assessed according to the concensus report from the Annapolis meeting on the mammary pathology of genetically engineered mice (27).

| Mouse | Tumor type | Age (days) |
|---|---|---|
| 1 | Mammary adenocarcinoma<br>*Solid tumor composed of sheets of epithelial cells with little or no glandular differentiation. Some differentiated ductal structures are visible in the periphery. The tumor is extensively infiltrated by lymphocytes.* | 384 |
| 2 | Hemangioma (near hind limb) | 475 |
| 3 | Mammary adenocarcinoma<br>*Solid tumor with distinct features. Some parts of the tumor are composed of small clusters reminiscent of glandular structures with small lumens. Other parts are composed of sheets of epithelial cells with little or no glandular differentiation. Some differentiated ductal structures are visible in the periphery.* | 558 |
| 4 | Mammary adenocarcinoma<br>*In the center the tumor is composed of sheets of solid cells with an undifferentiated appearance. Toward the periphery fairly differentiated small glandular clusters are present. Extensive fibrosis and lymphocyte infiltration can be seen. Some areas contain emerging squamous metaplasias.* | 608 |
| 5 | Mammary adenocarcinoma<br>*Solid tumor is composed of sheets of epithelial cells and nests of cells forming lumens.* | 763 |
| 6 | Stromal/sex cord tumor of the ovary | 770 |

tumors (18). These observations prompted us to study the status of p53 in adenocarcinomas from *Brca2*$^{fl9-10/fl9-10}$*; MMTV-Cre* mice. We performed immunohistochemistry using an antibody that recognizes p53 and found that three of four tumors examined failed to show normal staining for p53 protein (Fig. 4*B–G*). In cells of the adenocarcinoma of mouse 3 (Table 1 and Fig. 4, *B* and *C*), strong p53 staining occurred both in the cytoplasm and nucleus. In mouse 4, p53 was expressed in the nuclei (only) of all adenocarcinoma cells (Fig. 4, *D* and *E*). In mouse 1, there were no positively stained tumor cells (Fig. 4, *F* and *G*), suggesting that this adenocarcinoma had either completely lost p53 expression or that it retained undetectable levels of WT p53. [WT p53 is present in normal cells only at very low levels because of its rapid turnover (29).] The adenocarcinoma of mouse 5 exhibited an apparently normal pattern of p53 staining as p53 was present in the nucleus of only some of the tumor cells (data not shown).

Table 2 *p53 status in the four mammary adenocarcinomas from Brca2*$^{fl9-10/fl9-10}$*; MMTV-Cre mutant mice*

Microsequencing of *p53* exons 5–9 and immunohistochemistry (IHC) with an anti-p53 antibody were performed. No mut., no mutation found. In tumor case no. 3, a nucleotide transversion from G to T was detected at nucleotide position 888 (reference made to p53 cDNA clone GenBank accession no. 5081782). This tumor also demonstrated a strong positive staining of p53 in both cytoplasm (cyt.) and nucleus (nuc.) of tumor cells (Fig. 4*C*). Tumor case no. 1 showed negative (−) staining of p53 (Fig. 4*G*), case 4 showed positive staining in all tumor cell nuclei (Fig. 4*E*), and some cells in case no. 5 showed positive staining in their nuclei (data not shown).

| | p53 | |
|---|---|---|
| Tumor case no. | exon 5–9 sequencing | IHC staining |
| 1 | No mut. | − |
| 3 | 888 G → T | +++(cyt. +nuc.) |
| 4 | No mut. | +(nuc.) |
| 5 | No mut. | ±(nuc.) |

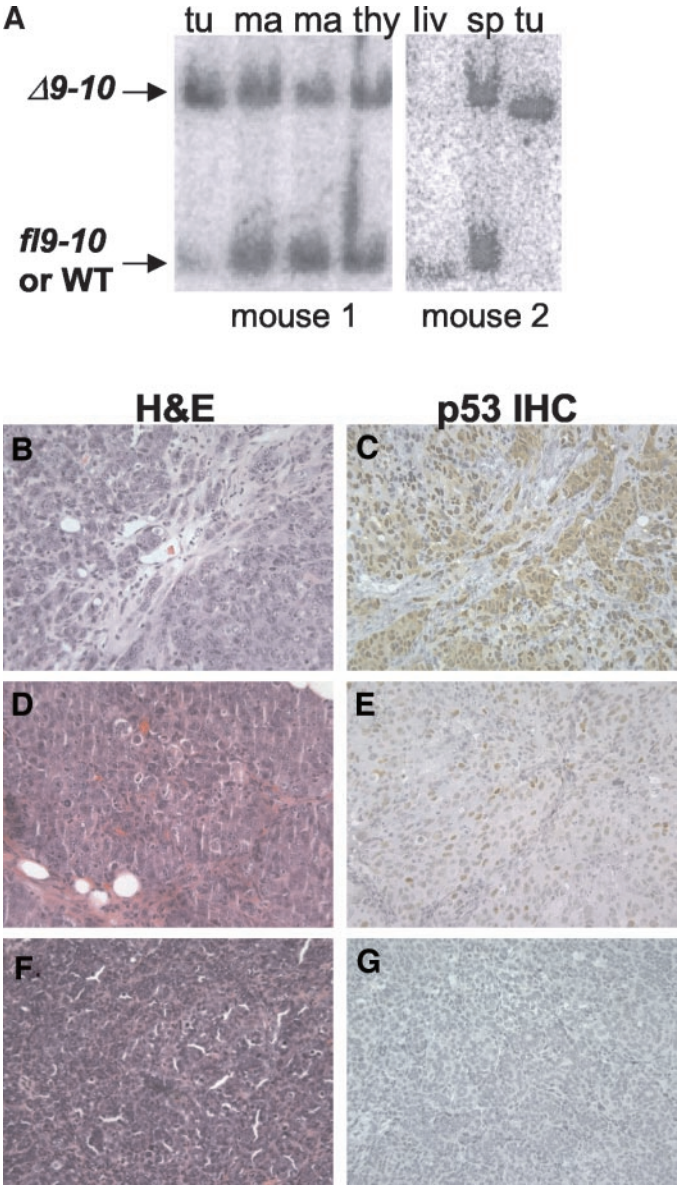


Fig. 4. Recombination of *Brca2*$^{fl9-10}$ and altered p53 protein expression in mammary adenocarcinomas from 2 *Brca2*$^{fl9-10/fl9-10}$*; MMTV-Cre* mice. *A*, Southern analysis of tumor cells (tu) from mammary adenocarcinomas of mouse 1 and mouse 2 showed near complete recombination of the *Brca2*$^{fl9-10}$ allele. Only partial recombination occurred in normal mammary tissue (ma), thymus (thy), liver (liv), or spleen (sp) of the same mutant mouse. *B*, *D*, and *F*, H&E staining of mammary adenocarcinomas from 3 *Brca2*$^{fl9-10/fl9-10}$*; MMTV-Cre* mice. *C*, *E*, and *G*, immunohistochemical analysis (IHC) of p53 expression in the tumors shown in *B*, *D*, and *F*, respectively.

To determine whether the *p53* gene was mutated in *Brca2*$^{fl9-10/fl9-10}$*; MMTV-Cre* adenocarcinomas, we used PCR to sequence *p53* exons 5–9 in either tumor genomic DNA or cDNA synthesized from tumor cell mRNA. Exons 5–9 of *p53* encode the sequence-specific DNA binding region, and the majority of mutations in human cancers is located in this region (30). As shown in Table 2, sequencing of multiple clones confirmed that one of four *Brca2*$^{fl9-10/fl9-10}$*; MMTV-Cre* adenocarcinomas exhibited a *p53* mutation. In tumor case 3, the G to T transversion at nucleotide 888 created a mutation from aspartate to tyrosine at residue 256 in the murine protein. This aspartate residue is conserved in WT human p53, and mutation to tyrosine has been found in human cancers (although it does not qualify as a mutation hot spot according to the online database of *p53* mutations available).[5] Interestingly, tumor case 3 displayed an abnormal p53 staining pattern (Fig. 4*C*), which could have resulted from this mutation. Mutations of *p53* have also been identified in lymphomas from mice with Brca2 truncation mutations. Cells from these animals displayed mutations of *p53* or other genes encoding proteins involved in cell cycle mitotic checkpoint regulation (31). Taken together, these results suggest that Brca2-mediated tumorigenesis can occur only after certain checkpoints are inactivated.

**Increased Incidence of Mammary Adenocarcinomas in Brca2$^{fl9-10/fl9-10}$; MMTV-Cre; p53$^{+/-}$ Mutants Compared with p53$^{+/-}$ Mice.** To determine whether down-regulation of p53 promoted tumorigenesis in mammary gland-specific Brca2-deficient mice, we compared the incidence and time of onset of mammary adenocarcinomas in mammary epithelium-specific Brca2-deficient *p53*$^{+/-}$ mice and control *p53*$^{+/-}$ mice. *p53*$^{+/-}$ mice spontaneously developed tumors such as osteosarcomas (the majority), lymphomas, and the occasional mammary adenocarcinoma, consistent with previous studies (24, 32). We performed Southern blotting of tumor cell genomic DNA obtained from five tumors of *Brca2*$^{fl9-10/fl9-10}$*; MMTV-Cre; p53*$^{+/-}$ or *Brca2*$^{fl9-10/fl9-10}$*; WAP-Cre*; *p53*$^{+/-}$ mice. In four of five tumors, in addition to the loss of Brca2 as indicated by the extensive recombination of *Brca2*$^{fl9-10}$ allele, loss of heterozygosity of the p53 locus had also occurred (Fig. 5*A*). A log-rank test was used to compare the survival curves of the different mutant lines. We detected only a marginal difference between the survival rates of *Brca2*$^{fl9-10/fl9-10}$*; MMTV-Cre; p53*$^{+/-}$ mutants (median survival of 310 days; $n = 9$) and *Brca2*$^{fl9-10/+}$*; MMTV-Cre; p53*$^{+/-}$ mice (median survival of 470 days; $n = 5$; $P = 0.0128$) or *p53*$^{+/-}$ mice (median survival of 385 days; $n = 11$; $P = 0.0113$; Fig. 5*B*). On the other hand, out of 15

[5] Internet address: http://www.iarc.fr/p53.

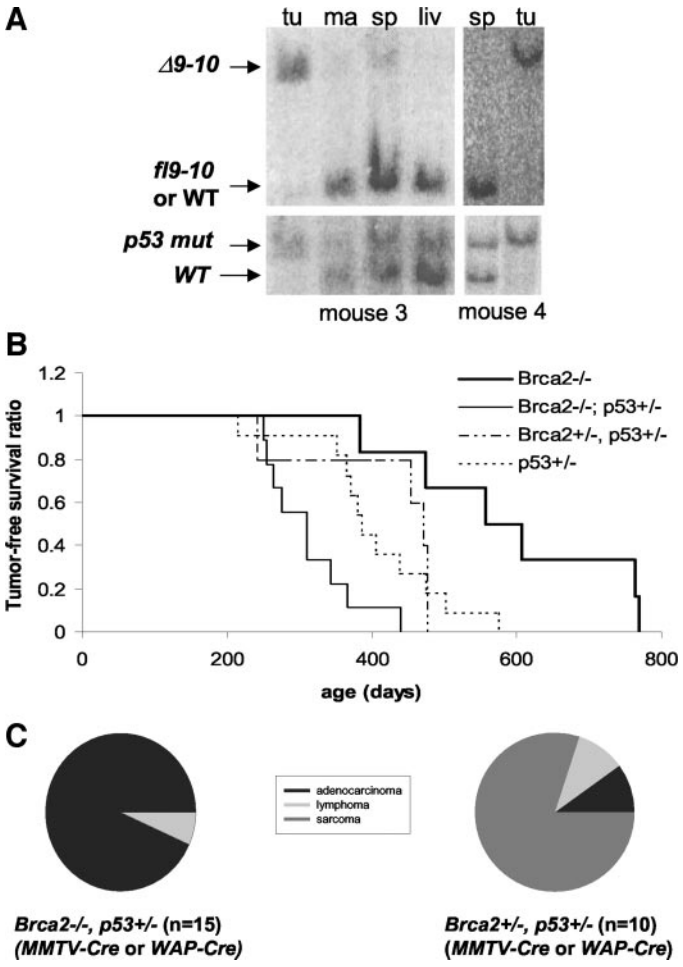


Fig. 5. Loss of heterozygosity of $p53^{+/-}$ and increased incidence of mammary adenocarcinomas in mammary gland-specific Brca2-deficient $p53^{+/-}$ mice. *A*, Southern blot of genomic DNA obtained from the tumors (tu) or normal mammary tissue (ma), spleen (sp), or liver (liv) of a $Brca2^{fl9-10/fl9-10}$; *WAP-Cre*; $p53^{+/-}$ mutant (mouse 3) and a $Brca2^{fl9-10/fl9-10}$; *MMTV-Cre*; $p53^{+/-}$ mutant (mouse 4). In addition to extensive recombination of the Brca2 *fl9–10* allele, the tumor cells have undergone loss of heterozygosity at the *p53* locus. *B*, Kaplan-Meyer analysis of the tumor-free survival of 6 $Brca2^{fl9-10/fl9-10}$; *MMTV-Cre* ($Brca2^{-/-}$) mice, 9 $Brca2^{fl9-10/fl9-10}$; *MMTV-Cre*; $p53^{+/-}$ ($Brca2^{-/-}$, $p53^{+/-}$) mice, 5 $Brca2^{fl9-10/+}$; *MMTV-Cre*; $p53^{+/-}$ ($Brca2^{+/-}$, $p53^{+/-}$) mice, and 11 $p53^{+/-}$ mice. *C*, pie chart representation of the spectrum of tumors developing in 15 $Brca2^{fl9-10/fl9-10}$; *MMTV-Cre*; $p53^{+/-}$ or $Brca2^{fl9-10/fl9-10}$; *WAP-Cre*; $p53^{+/-}$ ($Brca2^{-/-}$, $p53^{+/-}$, MMTV-Cre or WAP-Cre) mutant mice compared with 10 $Brca2^{fl9-10/+}$; *MMTV-Cre*; $p53^{+/-}$ or $Brca2^{fl9-10/+}$; *WAP-Cre*; $p53^{+/-}$ ($Brca2^{+/-}$, $p53^{+/-}$, MMTV-Cre, or WAP-Cre) controls.

$Brca2^{-/-}$; $p53^{+/-}$ ($Brca2^{fl9-10/fl9-10}$; *MMTV-Cre*; $p53^{+/-}$ or $Brca2^{fl9-10/fl9-10}$; *WAP-Cre*; $p53^{+/-}$) mutants examined, 14 (93%) developed mammary adenocarcinomas (Fig. 5*C*). In contrast, only 1 of 10 (10%) $Brca2^{+/-}$; $p53^{+/-}$ mice developed an adenocarcinoma, a difference that was statistically highly significant ($P < 0.0001$). These data indicate that the loss of Brca2 in mammary tissues greatly skewed tumor development toward mammary adenocarcinomas in $p53^{+/-}$ mice and suggest that Brca2 deficiency in the mammary epithelium strongly promotes tumorigenesis of this tissue when p53 function is deficient.

## DISCUSSION

The role of the breast cancer susceptibility gene Brca2 in DNA damage repair and Rad51 regulation is now well established. However, until this study, it was unknown whether Brca2 was required for the normal growth of mammary epithelial cells, particularly during pregnancy when extensive proliferation occurs to prepare the mammary gland for lactation. Our analyses indicate that an absence of Brca2 does not impair the expansion of mammary ducts or alveoli during pregnancy. Our data also imply that the potential accumulation of DNA breaks resulting from Brca2 deficiency does not induce a checkpoint for repair or apoptosis. Furthermore, although the mammary epithelium undergoes massive apoptosis during involution, there were no significant differences between mammary-specific Brca2-deficient mice and controls in the kinetics of apoptosis. In contrast, loss of Brca2 in proliferating T lymphocytes increases the level of spontaneous apoptosis (21), possibly through the up-regulation of the p53 target gene Bax (A. M. Y. Cheung and T. W. Mak, unpublished data). The basis for this tissue-specific difference is under investigation.

In agreement with previous studies (17), the loss of Brca2 in mammary glands enhances the development of spontaneous tumors. Inactivation of one WT p53 allele in mice homozygous for a mammary-specific Brca2 mutation significantly skewed the tumor spectrum toward the development of mammary adenocarcinomas. These data complement with the observation of Jonkers *et al.* (18) that mutations of Brca2 and p53 in myoepithelial cells have synergistic effects on breast cancer development. Although we previously demonstrated that T-cell-specific loss of Brca2 alone does not promote cancerous transformation of these cells, the loss of both Brca2 and p53 in T cells promotes the development of T-cell lymphomas (21). These data, together with the observation of apparently normal mammary tissue development in the absence of Brca2, strongly support the hypothesis that Brca2 functions as a mammary tissue-specific tumor suppressor.

DNA-damaging stress induces most cells to activate molecular checkpoints that induce either cell cycle arrest to allow for repair of the damage or apoptosis to eliminate the cell with genomic aberrations. However, stressed mammary epithelial and ovarian cells ignore these checkpoints and continue to propagate (33), perhaps because these cells are constantly exposed to survival signals from growth-promoting sex hormones that override the apoptotic signals. The unique hormonal milieu of female reproductive tissues may explain why mutations of the BRCA genes specifically promote tumorigenesis in these tissues. The identification of BRCA1's involvement in X chromosome inactivation also supports the biological importance of BRCA1 in female-restricted tissues (34). In contrast, BRCA2 mutations have been found in some breast cancers in males, suggesting that BRCA2 functions are tissue-specific rather than sex specific.

Certain genetic features are associated with hereditary BRCA breast tumors in humans. Besides being genetically unstable and exhibiting specific chromosomal gains or losses (35), mutations of *p53* have been found more frequently in BRCA1- or BRCA2-associated breast tumors than in sporadic breast cancers (28, 36, 37). Moreover, the spectrum of *p53* mutations in BRCA-deficient breast tumors is different from that found in sporadic cases (36). In mouse models, novel *p53* mutations were found in lymphomas of mice homozygous for Brca2 truncation mutations (31). Our own sequencing and immunohistochemical analyses of p53 mutations in spontaneous mammary adenocarcinomas from $Brca2^{fl9-10/fl9-10}$; *MMTV-cre* mice showed that the expression patterns of p53 protein were aberrant in three of four tumors.

Structural analyses have shown that the BRC4 region of BRCA2 binds to Rad51 (8) and that the COOH terminus of BRCA2 binds to single-stranded DNA (10). BRCA2 thus works locally with Rad51 and other binding partners to mediate repair of DNA double-strand break (38). However, the mechanism underlying the tissue specificity of BRCA2's role in tumor suppression remains a mystery. Our study has shown that, unlike the requirement of Brca1 for normal ductal tree expansion during pregnancy (25), Brca2 is not required for normal

mammary epithelium development. Nevertheless, a proportion of Brca1- and Brca2-deficient animals develop spontaneous mammary tumors after a long latency. It also remains unclear how and why the normal-looking mutant gland progresses toward the cancerous state. If proliferation and the subsequent accumulation of chromosomal aberrations in the mammary epithelium are indeed the forces driving tumorigenic transformation, it will be interesting to study whether the application of DNA-damaging agents or sex hormones such as estrogen and prolactin can accelerate the onset of tumorigenesis in Brca2-deficient animals.

## ACKNOWLEDGMENTS

We thank Rama Khokha for help with whole mount analysis; Kelvin So for histology and immunohistochemistry; Ivana Miljanic for DNA sequencing; James Woodgett and Sam Benchimol for critical comments; and Mary Saunders for scientific editing of the manuscript.

## REFERENCES

1. Miki Y, Swensen J, Shattuck-Eidens D, et al. A strong candidate for the breast and ovarian cancer susceptibility gene BRCA1. Science (Wash. DC) 1994;266:66–71.
2. Tavtigian SV, Simard J, Rommens J, et al. The complete BRCA2 gene and mutations in chromosome 13q-linked kindreds. Nat Genet 1996;12:333–7.
3. Rajan JV, Marquis ST, Gardner HP, Chodosh LA. Developmental expression of Brca2 colocalizes with Brca1 and is associated with proliferation and differentiation in multiple tissues. Dev Biol 1997;184:385–401.
4. Chodosh LA. Expression of BRCA1 and BRCA2 in normal and neoplastic cells. J Mammary Gland Biol Neoplasia 1998;3:389–402.
5. Sharan SK, Bradley A. Murine Brca2: sequence, map position, and expression pattern. Genomics 1997;40:234–41.
6. Jasin M. Homologous repair of DNA damage and tumorigenesis: the BRCA connection. Oncogene 2002;21:8981–93.
7. Moynahan ME, Pierce AJ, Jasin M. BRCA2 is required for homology-directed repair of chromosomal breaks. Mol Cell 2001;7:263–72.
8. Pellegrini L, Yu DS, Lo T, et al. Insights into DNA recombination from the structure of a RAD51-BRCA2 complex. Nature (Lond.) 2002;420:287–93.
9. Davies AA, Masson JY, McIlwraith MJ, et al. Role of BRCA2 in control of the RAD51 recombination and DNA repair protein. Mol Cell 2001;7:273–82.
10. Yang H, Jeffrey PD, Miller J, et al. BRCA2 function in DNA binding and recombination from a BRCA2-DSS1-ssDNA structure. Science (Wash. DC) 2002;297:1837–48.
11. Hughes-Davies L, Huntsman D, Ruas M, et al. EMSY links the BRCA2 pathway to sporadic breast and ovarian cancer. Cell 2003;115:523–35.
12. Patel KJ, Yu VP, Lee H, et al. Involvement of Brca2 in DNA repair. Mol Cell 1998;1:347–57.
13. Sharan SK, Morimatsu M, Albrecht U, et al. Embryonic lethality and radiation hypersensitivity mediated by Rad51 in mice lacking Brca2. Nature (Lond.) 1997;386:804–10.
14. Tutt A, Gabriel A, Bertwistle D, et al. Absence of Brca2 causes genome instability by chromosome breakage and loss associated with centrosome amplification. Curr Biol 1999;9:1107–10.
15. Yu VP, Koehler M, Steinlein C, et al. Gross chromosomal rearrangements and genetic exchange between nonhomologous chromosomes following BRCA2 inactivation. Genes Dev 2000;14:1400–6.
16. Ford D, Easton DF, Stratton M, et al. Genetic heterogeneity and penetrance analysis of the BRCA1 and BRCA2 genes in breast cancer families. The Breast Cancer Linkage Consortium Am J Hum Genet 1998;62:676–89.
17. Ludwig T, Fisher P, Murty V, Efstratiadis A. Development of mammary adenocarcinomas by tissue-specific knockout of Brca2 in mice. Oncogene 2001;20:3937–48.
18. Jonkers J, Meuwissen R, van der Gulden H, Peterse H, van der Valk M, Berns A. Synergistic tumor suppressor activity of BRCA2 and p53 in a conditional mouse model for breast cancer. Nat Genet 2001;29:418–25.
19. Hennighausen L, Robinson GW. Signaling pathways in mammary gland development. Dev Cell 2001;1:467–75.
20. Robinson GW, Hennighausen L, Johnson PF. Side-branching in the mammary gland: the progesterone-Wnt connection. Genes Dev 2000;14:889–94.
21. Cheung AM, Hande MP, Jalali F, et al. Loss of Brca2 and p53 synergistically promotes genomic instability and deregulation of T-cell apoptosis. Cancer Res 2002;62:6194–204.
22. Wagner KU, Wall RJ, St-Onge L, et al. Cre-mediated gene deletion in the mammary gland. Nucleic Acids Res 1997;25:4323–30.
23. Wagner KU, McAllister K, Ward T, Davis B, Wiseman R, Hennighausen L. Spatial and temporal expression of the Cre gene under the control of the MMTV-LTR in different lines of transgenic mice. Transgenic Res 2001;10:545–53.
24. Donehower LA, Harvey M, Slagle BL, et al. Mice deficient for p53 are developmentally normal but susceptible to spontaneous tumours. Nature (Lond.) 1992;356:215–21.
25. Xu X, Wagner KU, Larson D, et al. Conditional mutation of Brca1 in mammary epithelial cells results in blunted ductal morphogenesis and tumour formation. Nat Genet 1999;22:37–43.
26. Marti A, Ritter PM, Jager R, et al. Mouse mammary gland involution is associated with cytochrome *c* release and caspase activation. Mech Dev 2001;104:89–98.
27. Cardiff RD, Anver MR, Gusterson BA, et al. The mammary pathology of genetically engineered mice: the consensus report and recommendations from the Annapolis meeting. Oncogene 2000;19:968–88.
28. Crook T, Brooks LA, Crossland S, et al. p53 mutation with frequent novel condons but not a mutator phenotype in BRCA1- and BRCA2-associated breast tumours. Oncogene 1998;17:1681–9.
29. Haupt Y, Maya R, Kazaz A, Oren M. Mdm2 promotes the rapid degradation of p53. Nature (Lond.) 1997;387:296–9.
30. Hainaut P, Hollstein M. p53 and human cancer: the first ten thousand mutations. Adv Cancer Res 2000;77:81–137.
31. Lee H, Trainer AH, Friedman LS, et al. Mitotic checkpoint inactivation fosters transformation in cells lacking the breast cancer susceptibility gene, Brca2. Mol Cell 1999;4:1–10.
32. Jacks T, Remington L, Williams BO, et al. Tumor spectrum analysis in p53-mutant mice. Curr Biol 1994;4:1–7.
33. Elledge SJ, Amon A. The BRCA1 suppressor hypothesis: an explanation for the tissue-specific tumor development in BRCA1 patients. Cancer Cell 2002;1:129–32.
34. Ganesan S, Silver DP, Greenberg RA, et al. BRCA1 supports XIST RNA concentration on the inactive X chromosome. Cell 2002;111:393–405.
35. Tirkkonen M, Johannsson O, Agnarsson BA, et al. Distinct somatic genetic changes associated with tumor progression in carriers of BRCA1 and BRCA2 germ-line mutations. Cancer Res 1997;57:1222–7.
36. Smith PD, Crossland S, Parker G, et al. Novel p53 mutants selected in BRCA-associated tumours which dissociate transformation suppression from other wild-type p53 functions. Oncogene 1999;18:2451–9.
37. Greenblatt MS, Chappuis PO, Bond JP, Hamel N, Foulkes WD. TP53 mutations in breast cancer associated with BRCA1 or BRCA2 germ-line mutations: distinctive spectrum and structural distribution. Cancer Res 2001;61:4092–7.
38. Powell SN, Willers H, Xia F. BRCA2 Keeps Rad51 in line, high-fidelity homologous recombination prevents breast and ovarian cancer? Mol Cell 2002;10:1262–3.